Rare Met. (2013) 32(2):105–112
DOI 10.1007/s12598-013-0047-8

RARE METALS
www.editorialmanager.com/rmet

Advance in the chemical synthesis and magnetic properties of nanostructured rare-earth-based permanent magnets

Ce Yang, Yang-Long Hou*

Received: 11 March 2013 / Revised: 12 March 2013 / Accepted: 15 March 2013 / Published online: 23 April 2013

Abstract Rare-earth-based permanent magnets are one of the most important magnets in both scientific and industrial fields. With the development of technology, nanostructured rare-earth-based permanent magnets with high energy products are highly required. In this article, we will review the progress in chemical synthetic strategies of nanostructured rare-earth-based permanent magnets.

Keywords Rare-earth; Permanent magnets; Chemical synthesis

1 Introduction

The application of permanent magnets starts as early as ancient China, where people made compass with the use of magnetite as a raw material. When it comes to the modern age, which is an age of electricity, permanent magnet is taking an increasingly important role in the contemporary society. In our daily life for example, majority household appliances in a family contain certain amount of permanent magnets. Moreover, electric motor, which is a crucial part in a vehicle, also includes large volume of permanent magnets. Another example lies in the field of biomedical. With the permanent magnets as the working part, the Magnetic Resonance Imaging (MRI) machine will diagnose various diseases without any harm to the human body. Therefore, the demands for permanent magnets with larger maximum energy product $(BH)_{max}$, lighter weight, smaller volume, and higher working temperature are essential for the development of technologies nowadays.

The first influential finding in permanent magnets was Alnico 3(Al–Ni–Co–Fe alloy) by Honda and Mishima in early 1930s. The Alnico 3 possesses energy product about 8 $kJ{\cdot}m^{-3}$, which is superior than any other permanent magnet used before [1, 2]. Then, the discovery of ferrite hexagonal ferrites ($(Ba/Sr)Fe_{12}O_{19}$) increased the energy product into 24 $kJ{\cdot}m^{-3}$ [3]. However, these ferrite magnets hold small magnetization and low Curie temperatures. Following that, the most crucial step forward took place in 1960s, where the rare-earth-based permanent magnets were first realized as the form of RCo_5 intermetallics [4]. And this significantly enlarged the energy product of permanent magnets to 240 $kJ{\cdot}m^{-3}$, which is ten times larger than that of ferrite magnets. Afterward, in 1980s, the discovery of $Nd_2Fe_{14}B$ magnets further defined rare-earth-based magnets the most important permanent magnets [5–7]. The energy product of $Nd_2Fe_{14}B$ reaches as high as 392 $kJ{\cdot}m^{-3}$, and large content of Fe makes the magnets comparatively cheaper than the previous $SmCo_5$ magnets. Nevertheless, the lower Curie temperature ($\sim$573 K) is a major problem of $Nd_2Fe_{14}B$. In order to look for a new generation of permanent magnets which hold even higher energy product and Curie temperature, in 1990s, researchers proposed the model for the hard/soft phase exchange-coupled magnets [8]. According to the simulation result, the theoretical energy product for $Nd_2Fe_{14}B/Fe$ exchange magnet is 960 $kJ{\cdot}m^{-3}$. However, results which recently reported still have big gap between the simulation ones.

Having realized its importance, scientist developed various methods to prepare rare-earth-based magnets. And among them, chemical route is considered one of the major strategies. Especially with the trends of miniaturization and

C. Yang, Y.-L. Hou*
Department of Materials Science and Engineering, College of Engineering, Peking University, Beijing 100871, China
e-mail: hou@pku.edu.cn

integration in current industrial world, chemical synthesis provides an easy way to tune size and composition of magnets so that the as-synthesized permanent magnets will meet the requirement of application. In this review, we will describe the progress in chemical synthesis of various nanostructured rare-earth-based permanent magnets as well as their magnetic properties. And we will also provide a view for the bottlenecks as well as futures of the chemical method.

2 Chemical synthesis of Sm–Co permanent magnets

As mentioned above, Sm–Co magnets were the first investigated rare-earth-based permanent magnets. The consisting of only two elements in Sm–Co magnets make them comparatively easier to prepare than three-elements magnets such as Sm–Fe–N or Nd–Fe–B. Therefore, the chemical synthetic strategies of Sm–Co magnets have been intensively investigated over years aiming to find an approach to make Sm–Co magnets with high energy product, tunable size, and excellent stability [9–24]. In the early days, researchers attempted to synthesize Sm–Co nanoparticles (NPs) directly from wet chemical method since it is the most accepted way to control the morphology of NPs [9]. However, people soon found that the electronegativity and reactivity of Sm make it extremely difficult. Thus, a high temperature reductive annealing with Ca as reducing agent is introduced in the chemical synthesis of rare-earth-based permanent magnets [13, 20].

Hou et al. [13] synthesized $SmCo_5$ magnets with nanoscale domains from core/shell Co/Sm_2O_3 NPs. According to their route, they initially prepared 8 nm-sized Co NPs via decomposition of $Co_2(CO)_8$ in mixture of oleic acid, dioctylamine, and tetralin under ambient atmosphere (Fig. 1a). The obtained 8 nm Co NPs were dispersed in hexne and subsequently injected in mixture of oleylamine and oleic acid with $Sm(acac)_3$ dissolved in. The system was then heated to 250 °C to trigger decomposition of Sm $(acac)_3$ on the surface of Co NPs and core/shell Co/Sm_2O_3 NPs were generated (Fig. 1b). Later, the $SmCo_5$ magnets were fabricated by reductive annealing of as-synthesized Co/Sm_2O_3 NPs under 900 °C in Ar/H_2 with metallic Ca as reducing agent and KCl as solvent. According to the HRTEM image, the acquired $SmCo_5$ magnets are assembled by nanoscale domains with various orientations with a lattice space of 0.293 nm (Fig. 1c). The magnets exhibit coercivity of 0.8 T and remnant magnetic moment of 40–50 $A{\cdot}m^2{\cdot}kg^{-1}$ under room temperature. Moreover, the researchers showed that the same strategy can be applied in the preparation of Sm_2Co_{17} by tune the Sm/Co ratio during the synthesis of Co/Sm_2O_3 NPs (Fig. 1d).

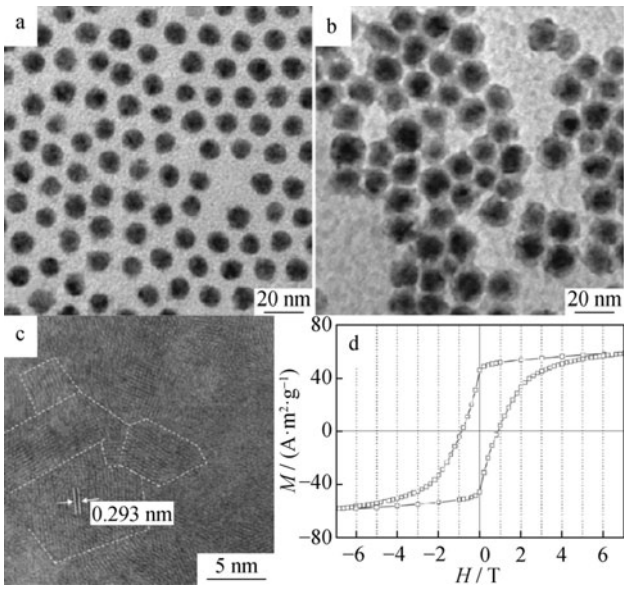

Fig. 1 **a** TEM images of Co NPs with size of 8 nm, **b** TEM image of Co/Sm_2O_3 NPs, **c** HRTEM of as-synthesized $SmCo_5$ magnet with assembles of nanocrystals as indicated by *dashlines*, and **d** hysteresis loops of $SmCo_5$ under room temperature. Reproduced with permission from Ref. [13]. Copyright 2007 John Wiley & Sons

Following the strategy developed by Hou et al., Zhang et al. [20, 25] further synthesized 6 nm monodispersed $SmCo_5$ NPs. In their method, 7 nm monodispersed Sm–Co–O embedded in CaO matrix was first prepared by co-decomposition of $Co(ac)_2$ and $Sm(ac)_3$ in *n*-hexadecyltrimethylammonium hydroxide (HTMA–OH) with the presence of $Ca(ac)_2$. And the decomposition of $Ca(ac)_2$ led to the formation of CaO matrix which embraced Sm–Co–O and hence would inhibit the diffusion of $SmCo_5$ under annealing temperature (Fig. 2a). Afterward, the Sm–Co–O@CaO composite was annealed under 960 °C for 2 h in Ar/H_2 with Ca as reducing agent and KCl as solvent. According to XRD patterns and TEM images, the resultant was $SmCo_5$ NPs embedded in CaO matrix. After removal of CaO matrix by washing in ethanol and deionized (DI) water, the as-synthesized $SmCo_5$ NPs showed narrow size distribution and diameter of 6 nm, which was quite similar to that of Sm–Co–O NPs (Fig. 2c–e). This $SmCo_5$ NPs exhibit reduced coercivity of 0.72 T and remnant magnetic moment of 35 $A{\cdot}m^2{\cdot}kg^{-1}$. In addition to that, the researchers also employed this method to synthesize Sm_2Co_{17} NPs, and the coercivity as well as remnant magnetization were 0.58 T and 45 $A{\cdot}m^2{\cdot}kg^{-1}$, respectively. So far, this method is the most controllable chemical route in terms of composition and morphology. However, the as-synthesized Sm–Co NPs are so reactive that they will be rapidly oxidized and thus lose their magnetic properties if exposed to air.

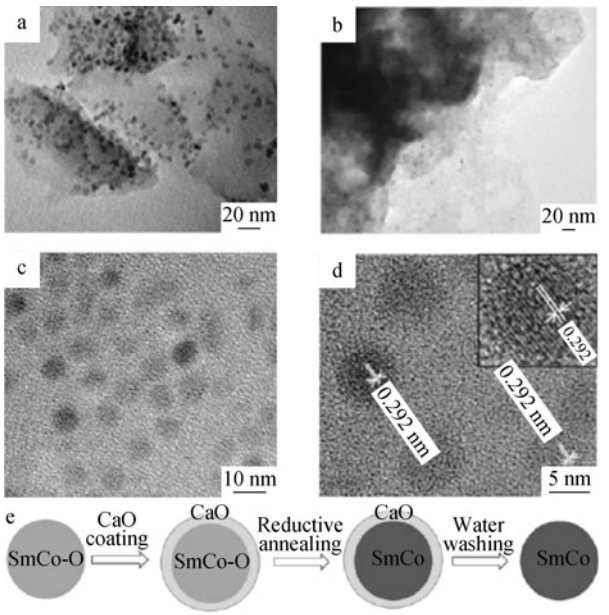

Fig. 2 **a** TEM image of the 7 nm $SmCo_{3.6}$–O NPs in the CaO matrix, **b** TEM images for $SmCo_5$ NPs in CaO matrix after annealing, **c** TEM images for the 6 nm $SmCo_5$ NPs after removal of CaO matrix, **d** HRTEM image of the $SmCo_5$ NPs, and **e** Schemes for the synthetic route of Sm–Co NPs. Reproduced with permission from Ref. [25]. Copyright 2013 IOP Publishing Ltd

Surfactant assisted ball milling (SABM) is another popular method to synthesize nanostructured Sm–Co magnets [11, 14, 18, 19, 26]. According to the reports, oleic acid and oleylamine are the most commonly used surfactants in the high energy ball milling of Sm–Co magnets [17, 18, 25]. Surfactant will prevent the fragmentized NPs from re-welding. In addition to that, surfactant will also help the dispersion of NPs so that they will not aggregate. Poudyal et al. [18] synthesized $SmCo_x$ ($x = 3.5$, 4.0, 5.0, 6.0, 8.5, and 10.0) NPs via SABM technique. In their process, they prepared $SmCo_x$ magnetic powders via arc melting and the following grinding process. The as-synthesized $SmCo_x$ powders were transferred into a mixture of heptane, oleic acid, and oleylamine for ball milling. After milling for 20 h, the products were taken out under ambient atmosphere and went through a size selection process. (That is to separate NPs of various sizes by tune the sedimentary time of the mixture.) According to the TEM images, 6 nm, 20 nm, and submicron Sm_2Co_{17} particles were received by collecting the deposition after different sedimentary time (Fig. 3a–c). The XRD diffraction peaks of 20 nm and submicron-sized Sm_2Co_{17} NPs are broadened which indicated the reduction of the grain size in both samples. However, the XRD pattern of 6 nm NPs is one broad peak which implied the amorphous character of the 6 nm Sm_2Co_{17} NPs (Fig. 3d). In order to investigate the magnetic properties of the $SmCo_x$ NPs made from SABM, researchers tuned the composition of $SmCo_x$ and made a series of $SmCo_x$ NPs ($x = 3.5$, 4.0, 5.0, 6.0, 8.5, and 10.0). With various Sm/Co ratio, researchers noticed that the coercivity of the as-synthesized $SmCo_x$ NPs vary from 0.05 to 0.3 T (Fig. 3e).

Yue et al. [24] also utilized SABM method and a subsequently size selection process to prepare $SmCo_5$ NPs and nanoflakes with high coercivity and narrow size distributions. The $SmCo_5$ NPs have average p sizes of 9.8 and 47.5 nm, and they exhibit coercivity values of 6.8×10^4 and 7.3×10^5 $A{\cdot}m^{-1}$ under room temperature. Moreover, the $SmCo_5$ nanoflakes have diameter about 1.4 μm and average thickness of 75 nm. The researchers found that the $SmCo_5$ nanoflakes present strong magnetic anisotropy. The coercivity along easy-axis is 5.5×10^5 $A{\cdot}m^{-1}$, while the coercivity along hard-axis is 1.6×10^6 $A{\cdot}m^{-1}$.

3 Chemical synthesis of Nd–Fe–B permanent magnets

As mentioned in the synthesis of Sm–Co NPs, researchers originally tried to use wet chemical route to directly generate $Nd_2Fe_{14}B$ NPs with controllable size and pure phase [25, 27]. However, all the attempts failed due to the high negative reduction potential of Nd. Moreover, the bottom-up strategies which were described in preparation of Sm–Co NPs are unsuitable ascribe to the nature that $Nd_2Fe_{14}B$ consisted of three elements rather than two. Therefore, sol–gel and SABM are the widely employed method to synthesize $Nd_2Fe_{14}B$ NPs [11, 16, 19, 23, 28–32].

Deheri et al. [30] synthesized $Nd_2Fe_{14}B$ via sol–gel-based chemical methods. In their process, $NdCl_3$, $FeCl_3$, and boric acid were used as the source of Nd, Fe, and B, respectively. In addition to that, citric acid and ethylene glycol were employed as crosslinking agent and solvent. The Nd–Fe–B–O was prepared by modified Pechini type sol–gel method. Then, $Nd_2Fe_{14}B$ NPs were obtained by annealing the Nd–Fe–B–O powders under 800 °C in N_2 atmosphere with CaH_2 as reduction agent. According to the XRD characterization, the major phase of the resultant is $Nd_2Fe_{14}B$, while some impurities such as $Nd_2Fe_{14}BH_{4.7}$(27.68 %) and α-Fe (2.43 %) were also detected (Fig. 4a). The TEM image suggested that the $Nd_2Fe_{14}B$ NPs are highly aggregate with average size of 50 nm, (Fig. 4b) and the hysteresis loop characterized by VSM under room temperature showed that the obtained $Nd_2Fe_{14}B$ NPs have saturation magnetization of 102.3 $A{\cdot}m^2{\cdot}kg^{-1}$ and decreased coercivity of 0.39 T (Fig. 4c). The big gap of the magnetic property between as-synthesized $Nd_2Fe_{14}B$ NPs and bulk $Nd_2Fe_{14}B$ magnet is probably caused by the impurity as well as minimization of the grain size. In a subsequent work from Deheri et al. [31], they further looked into the mechanism of the transformation from Nd–Fe–B-oxide to $Nd_2Fe_{14}B$ NPs. And they

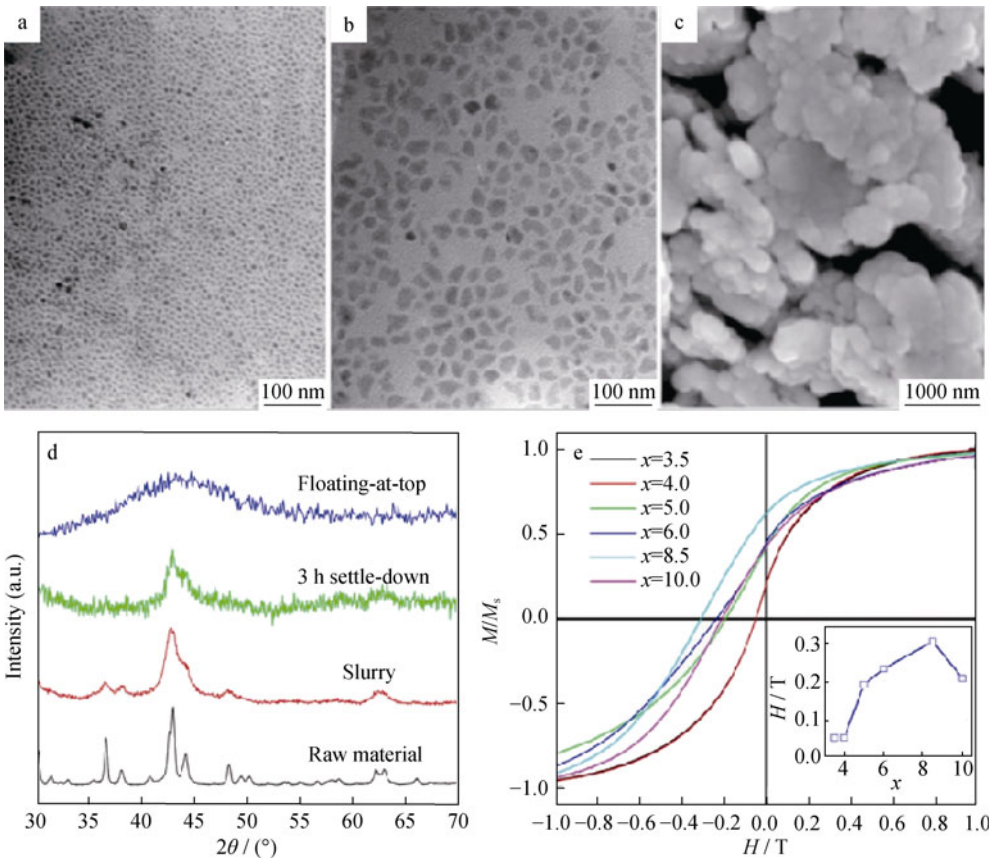

Fig. 3 **a** TEM images of 6 nm Sm_2Co_{17} NPs, **b** TEM images of 20 nm Sm_2Co_{17} NPs, **c** SEM image of submicron Sm_2Co_{17} particles, **d** XRD patterns of the as-synthesized Sm_2Co_{17} NPs and raw material, and **e** demagnetization curves of the Sm–Co NPs with various composition. The *inset* illustrating the relationship between composition and coercivity of the SmCo NPs. Reproduced with permission from Ref. [18]. Copyright 2010 American Institute of Physics

provided the following conclusions: (1) Reduction–diffusion consisted of three steps. Initially, Fe_2O_3 and B_2O_3 will be reduced to Fe and B at 300 °C. Then, Nd_2O_3 and $NdFeO_3$ will be reduced and hydrogenated to NdH_2 and Fe at 620°. Finally, $Nd_2Fe_{14}B$ phase will be formed at 692°. (2) Two parallel reactions were competing during the formation of $Nd_2Fe_{14}B$ NPs. The first one was the direct combination of NdH_2, Fe, and B to form $Nd_2Fe_{14}B$. The second one was the combination of NdH_2 and Fe to form Nd_2Fe_{17} followed by the reaction between Nd_2Fe_{17} and B to form $Nd_2Fe_{14}B$.

Due to the difficulty of preparing a single-phased Nd–Fe–B magnet by bottom-up strategy, researchers considered SABM as a more practical way to prepare nano-sized Nd–Fe–B particles [11, 19, 23, 28, 29, 32]. Akdogan et al. [29] synthesized $Nd_2Fe_{14}B$ alloy from arc-melting method as raw material. The $Nd_2Fe_{14}B$ powders were pre-milled in heptane for 4 h. Then, the slurry was further milled in the mixture of heptane and oleic acid for another 6 h. Finally, the obtained $Nd_2Fe_{14}B$ NPs were field-aligned. According to the XRD study, although the SABM leads to the broadening of the XRD peaks, the as-synthesized NPs exhibit pure phased tetragonal $Nd_2Fe_{14}B$ phase (Fig. 5a (1) and (2)). Moreover, XRD patterns of the field-aligned samples indicated [001] out-of-plane texture in $Nd_2Fe_{14}B$ NPs (Fig. 5a (3)). TEM image of the upper part of the slurry suggested that the generated $Nd_2Fe_{14}B$ NPs have square morphology with average size of 12 nm (Fig. 5b). The hysteresis loop of the square $Nd_2Fe_{14}B$ NPs showed that the coercivity of the sample is 0.18 T under room temperature and 0.4 T under 40 K (Fig. 5c).

Yue et al. [32] synthesized $Nd_2Fe_{14}B$ nanoflakes through SABM method. According to their results, the nanoflakes have average thickness of several tens nm and average diameter of 500–1,000 nm, and this shape anisotropy leads to a strong c-axis texture in the as-synthesized $Nd_2Fe_{14}B$ nanoflakes.

4 Chemical synthesis of hard/soft exchange-coupled permanent magnets

Since the first model of exchange-coupling effect was introduced by Coey et al., there have been intense interests on this effect which only takes place at interphase between hard

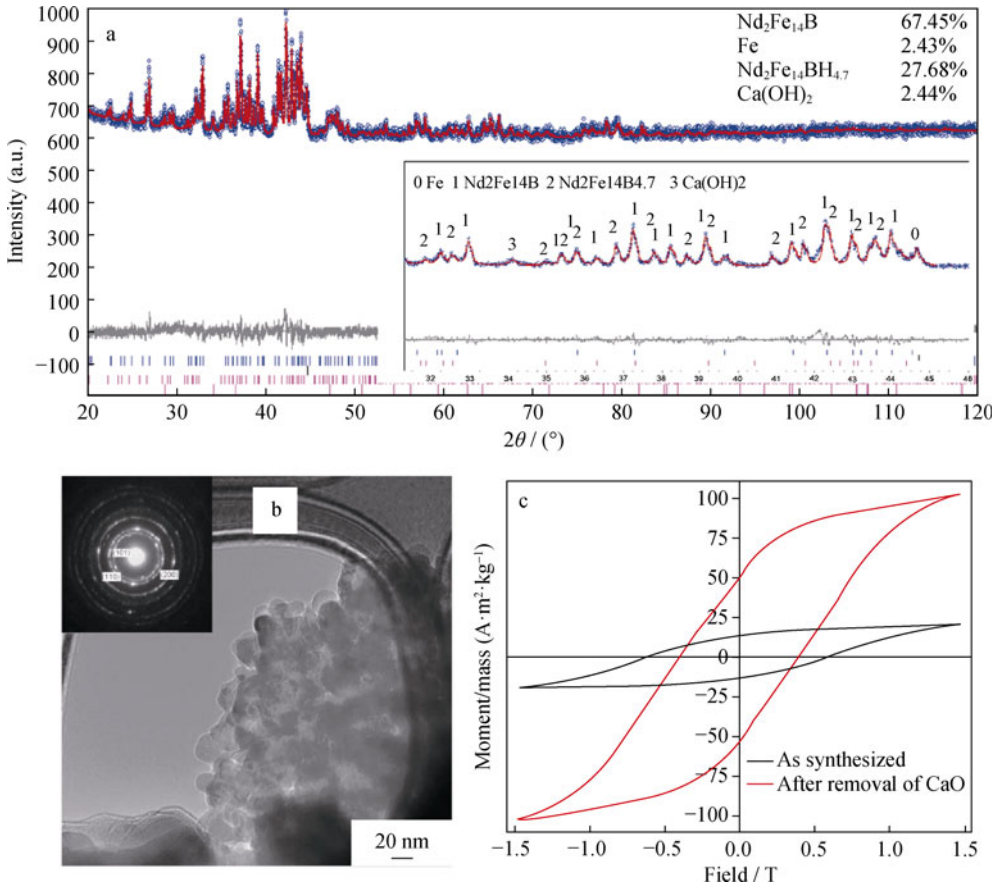

Fig. 4 **a** XRD pattern of as-synthesized $Nd_2Fe_{14}B$ NPs (*Inset* showing that peaks corresponding to $Nd_2Fe_{14}BH_{4.7}$ phase shifting to a lower 2θ compared with the XRD pattern of $Nd_2Fe_{14}B$.), **b** TEM image of as-synthesized $Nd_2Fe_{14}B$ NPs (*Inset* being the SADP of the NPs), and **c** hysteresis loop of as-synthesized $Nd_2Fe_{14}B$ NPs. Reproduced with permission from Ref. [30]. Copyright 2010 American Chemical Society

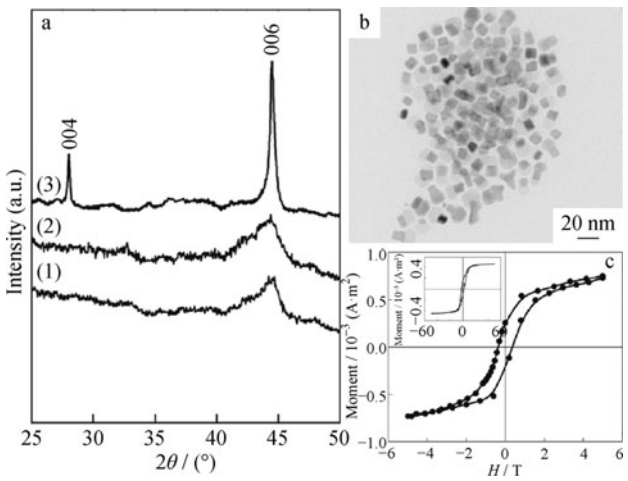

Fig. 5 **a** XRD patterns of $Nd_2Fe_{14}B$: (1) milled for 4 h in heptane, (2) milled for extra 6 h with OA, (3) after field-aligned for the 6 h milling; **b** TEM image of the upper part of the slurry; **c** hysteresis loop of square $Nd_2Fe_{14}B$ NPs at 40 K and room temperature (*Inset*). Reproduced with permission from Ref. [29]. Copyright 2010 IOP Publishing Ltd

and soft magnet in the range of nanosize. This exchange-coupled magnet can be designed according to the required properties by selecting different hard and soft phases and by tuning the phase ratio. Therefore, nanocomposite magnets have suggested new chances for the development of new generations of permanent magnets. Physical method, especially physical vapor deposition (PVD), is a more adopted method that scientists used to research the exchange-coupling effect. Through PVD method, one can easily change the phase composition as well as tune the phase ratio [33, 34]. However, PVD route cannot prepare magnets with high-yield. Therefore, based on the early results from PVD experiments as well as theoretical simulations, researchers have been trying to synthesize exchange-coupled magnets through chemical routes over decades [35–53]. However, it was never easy as the case in the PVD method.

Hou et al. [41] employed a wet chemical process and a following Ca reduction to synthesize $SmCo_5$/Fe exchange-coupled nanocomposite. In their strategy, Fe_3O_4/SmCo-hydroxide composite was first generated from precipitation

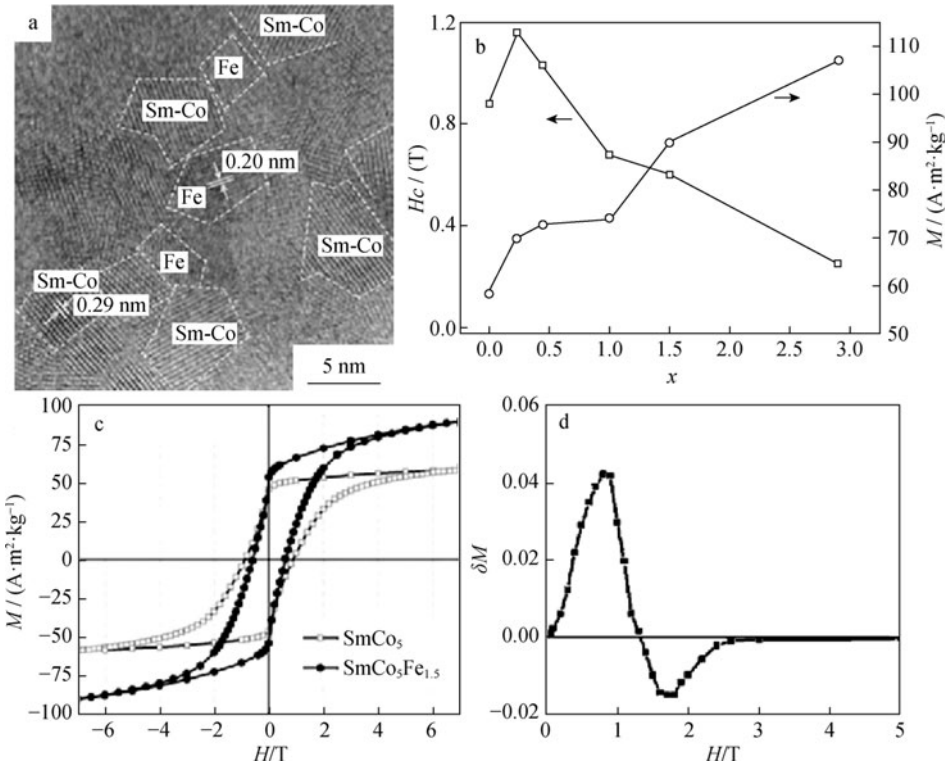

Fig. 6 **a** HRTEM of $SmCo_5$/Fe nanocomposite, **b** Change of coercivity and magnetic moment with various Fe ration in the $SmCo_5/Fe_x$, **c** Hysteresis loop of $SmCo_5$ and $SmCo_5/Fe_{1.5}$ magnets, and **d** δM–H plot of $SmCo_5/Fe_{1.5}$ magnet. Reproduced with permission from Ref. [41]. Copyright 2007 American Institute of Physics

of Sm and Co in monodispersed Fe_3O_4 NPs solutions. The Fe_3O_4 NPs were embedded in SmCo-hydroxide matrix, and this matrix could prevent Fe NPs from aggregation in the following reductive process. Afterward, the composites were annealed at 900 °C temperature for 1 h with Ca as reducing agent and KCl as dispersion medium. According to the HRTEM image, the average grain sizes of $SmCo_5$ and α-Fe are 29 nm and 8 nm, respectively (Fig. 6a). The researchers prepared a series of $SmCo_5/Fe_x$ ($x = 0$–2.9) samples, and found that both saturated magnetization and coercivity are varied with Fe content (Fig. 6b). The hysteresis loop of representative $SmCo_5/Fe_{1.5}$ showed enhanced saturated magnetization and single-phase behavior which implied the incorporation of soft phase α-Fe into hard phase $SmCo_5$ (Fig. 6c). The δ–M plot of the composition is initially positive, suggesting the existence of exchange coupling, but it soon drop to negative after the reversal, indicating magnetostatic interactions in the composite due to the presence of soft magnetic Fe phase (Fig. 6d).

5 Conclusion and perspectives

In summary, we have presented various chemical synthetic strategies to prepare nanostructured rare-earth-based permanent magnets. The chemical routes not only provide convenient approaches to prepare rare-earth-based permanent magnetic NPs but also offer an opportunity to manipulate the phase and morphology of the NPs to meet the requirement of current applications. However, there are still big challenges in the future development of chemical synthesis of nanostructured rare-earth-based permanent magnets. For example, the defects and impurities are often discovered in the NPs, and the particle morphology is relatively hard to control compared to non-rare-earth-based magnetic NPs. The as-synthesized NPs are too reactive to be practically stabilized. In the future, the proper use of other middle or heavy weight rare-earth elements might reduce the cost or enhance the magnetic properties of Sm- and Nd-based nanostructured magnets. In the case of bulk magnets, although single-phased Pr-, Te-, or Dy-based magnets exhibit either low anisotropy or small moment, the incorporation of those elements in Sm- or Nd-based magnets can dramatically increase the energy product of magnets [54–59]. In addition to that, the synthesis of rare-earth-based magnetic NPs with the composition other than RCo_x or RFeB was rarely reported. For example, Sm–Fe–N or Sm–Fe–C magnets also possess favorable magnetic property, while their nanostructures were seldom suggested. Moreover, the chemical synthesis of exchange-

coupled magnets still remains a big challenge. The current strategy is far from the objective of thoroughly controlling the composition and ratio in both hard and soft phase. Generally, the chemical method has great importance in the development of rare-earth-based magnetic NPs, and it needs to be further investigated in the coming years.

Acknowledgments This study was financially supported by the National Basic Research Program of China (No.2010CB934601), the National Natural Science Foundation of China (NSFC) (Nos. 51125001, 51172005, and 90922033), the Doctoral Program (No.20120001110078), and the Natural Science Foundation of Beijing (No. 2122022).

References

[1] Strnat KJ. Modern permanent-magnets for applications in electrotechnology. Proc IEEE. 1990;78(6):923.
[2] Cronk ER. Recent developments in high-energy alnico alloys. J Appl Phys. 1966;37(3):1097.
[3] Cochardt A. Recent ferrite magnet developments. J Appl Phys. 1966;37(3):1112.
[4] Strnat K, Hoffer G, Olson J, Ostertag W, Becker JJ. A family of new cobalt-base permanent magnet materials. J Appl Phys. 1967;38(3):1001.
[5] Sagawa M, Fujimura S, Togawa N, Yamamoto H, Matsuura Y. New material for permanent-magnets on a base of Nd and Fe. J Appl Phys. 1984;55(6):2083.
[6] Croat JJ, Herbst JF, Lee RW, Pinkerton FE. Pr–Fe and Nd–Fe based materials—a new class of high-performance permanent-magnets. J Appl Phys. 1984;55(6):2078.
[7] Herbst JF, Croat JJ. Magnetization of R_6Fe_{23} intermetallic compounds—molecular-field theory analysis. J Appl Phys. 1984;55(8):3023.
[8] Kneller EF, Hawig R. The exchange–spring magnet—a new material principle for permanent-magnets. IEEE Trans Magn. 1991;27(4):3588.
[9] Gu HW, Xu B, Rao JC, Zheng RK, Zhang XX, Fung KK, Wong CYC. Chemical synthesis of narrowly dispersed $SmCo_5$ nanoparticles. J Appl Phys. 2003;93(10):7589.
[10] Gu HW, Zheng RK, Rao JC, Zhang XX, Fung KK, Xu B. Chemical synthesis and magnetization measurement of $SmCo_5$ magnetic nanoparticles. Abstr Am Chem Soc. 2003;225:U74.
[11] Chakka VM, Altuncevahir B, Jin ZQ, Li Y, Liu JP. Magnetic nanoparticles produced by surfactant-assisted ball milling. J Appl Phys. 2006;99(8):08E912.
[12] Rong CB, Zhang HW, Chen RJ, Shen BG, He SL, Liu JP. Effects of annealing on the coercivity of $Sm(Co, Fe, Cu, Zr)_z$ ribbons and its temperature dependence. J Phys D Appl Phys. 2006;39(3):437.
[13] Hou YL, Xu ZC, Peng S, Rong CB, Liu JP, Sun SH. A facile synthesis of $SmCo_5$ magnets from core/shell Co/Sm_2O_3 nanoparticles. Adv Mater. 2007;19(20):3349.
[14] Wang YP, Li Y, Rong CB, Liu JP. Sm–Co hard magnetic nanoparticles prepared by surfactant-assisted ball milling. Nanotechnology. 2007;18(46):465701.
[15] Li Y, Zhang XL, Qiu R, Kang YS. Synthesis and investigation of $SmCo_5$ magnetic nanoparticles. Colloid Surf A Physicochem Eng Asp. 2008;313:621.
[16] Liu JP. Ferromagnetic nanoparticles: synthesis, processing, and characterization. JOM. 2010;62(4):56.
[17] Matsushita T, Iwamoto T, Inokuchi M, Toshima N. Novel ferromagnetic materials of $SmCo_5$ nanoparticles in single-nanometer size: chemical syntheses and characterizations. Nanotechnology. 2010;21(9):095603.
[18] Poudyal N, Rong CB, Liu JP. Effects of particle size and composition on coercivity of Sm–Co nanoparticles prepared by surfactant-assisted ball milling. J Appl Phys. 2010;107(9):09A703.
[19] Poudyal N, Nguyen VV, Rong CB, Liu JP. Anisotropic bonded magnets fabricated via surfactant-assisted ball milling and magnetic-field processing. J Phys D Appl Phys. 2011;44(33):335002.
[20] Zhang HW, Peng S, Rong CB, Liu JP, Zhang Y, Kramer MJ, Sun SH. Chemical synthesis of hard magnetic SmCo nanoparticles. J Mater Chem. 2011;21(42):16873.
[21] Suresh G, Saravanan P, Babu DR. Effect of annealing on phase composition, structural and magnetic properties of Sm–Co based nanomagnetic material synthesized by sol–gel process. J Magn Magn Mater. 2012;324(13):2158.
[22] Zheng LY, Cui BZ, Li WF, Hadjipanayis GC. Separated Sm–Co hard nanoparticles by an optimization of mechanochemical processes. J Appl Phys. 2012;7:07B536.
[23] Poudyal N, Altuncevahir B, Chakka V, Chen KH, Black TD, Liu JP, Ding Y, Wang ZL. Field-ball milling induced anisotropy in magnetic particles. J Phys D Appl Phys. 2004;37(24):L45.
[24] Zheng LY, Cui BZ, Zhao LX, Li WF, Hadjipanayis GC. Sm_2Co_{17} nanoparticles synthesized by surfactant-assisted high energy ball milling. J Alloys Compd. 2012;539:69.
[25] Poudyal N, Liu JP. Advances in nanostructured permanent magnets research. J Phys D Appl Phys. 2013;46(4):043001.
[26] Liu RM, Yue M, Zhang DT, Liu WQ, Zhang JX. Preparation, structure and magnetic properties of $SmCo_5$ nanoparticles and nanoflakes. Acta Metall Sin. 2012;48(4):475.
[27] Jadhav AP, Hussain A, Lee JH, Baek YK, Choi CJ, Kang YS. One pot synthesis of hard phase $Nd_2Fe_{14}B$ nanoparticles and $Nd_2Fe_{14}B$/alpha-Fe nanocomposite magnetic materials. New J Chem. 2012;36(11):2405.
[28] Yue M, Wang YP, Poudyal N, Rong CB, Liu JP. Preparation of Nd–Fe–B nanoparticles by surfactant-assisted ball milling technique. J Appl Phys. 2009;105(7):07A708.
[29] Akdogan NG, Hadjipanayis GC, Sellmyer DJ. Novel $Nd_2Fe_{14}B$ nanoflakes and nanoparticles for the development of high energy nanocomposite magnets. Nanotechnology. 2010;21(29):295705.
[30] Deheri PK, Swaminathan V, Bhame SD, Liu ZW, Ramanujan RV. Sol–gel based chemical synthesis of $Nd_2Fe_{14}B$ hard magnetic nanoparticles. Chem Mater. 2010;22(24):6509.
[31] Deheri PK, Shukla S, Ramanujan RV. The reaction mechanism of formation of chemically synthesized $Nd_2Fe_{14}B$ hard magnetic nanoparticles. J Solid State Chem. 2012;186:224.
[32] Yue M, Pan R, Liu RM, Liu WQ, Zhang DT, Zhang JX, Zhang XF, Guo ZH, Li W. Crystallographic alignment evolution and magnetic properties of Nd–Fe–B nanoflakes prepared by surfactant-assisted ball milling. J Appl Phys. 2012;111(7):07A732.
[33] Liu W, Zhang ZD, Liu JP, Chen LJ, He LL, Liu Y, Sun XK, Sellmyer DJ. Exchange coupling and remanence enhancement in nanocomposite multilayer magnets. Adv Mater. 2002;14(24):1832.
[34] Cui WB, Takahashi YK, Hono K. $Nd_2Fe_{14}B$/FeCo anisotropic nanocomposite films with a large maximum energy product. Adv Mater. 2012;24(48):6530.
[35] Cui BZ, Han K, Garmestani H, Su JH, Schneider-Muntau HJ, Liu JP. Enhancement of exchange coupling and hard magnetic properties in nanocomposites by magnetic annealing. Acta Mater. 2005;53(15):4155.
[36] Jiang JS, Pearson JE, Liu ZY, Kabius B, Trasobares S, Miller DJ, Bader SD, Lee, Haskel D, Srajer G, Liu JP. A new approach for improving exchange-spring magnets. J Appl Phys. 2005;97(10):10K311.

[37] Yu MH, Hattrick-Simpers J, Takeuchi I, Li J, Wang ZL, Liu JP, Lofland SE, Tyagi S, Freeland JW, Giubertoni D, Bersani M, Anderle M. Interphase exchange coupling in Fe/Sm–Co bilayers with gradient Fe thickness. J Appl Phys. 2005;98(6):063908.
[38] Liu S, Higgins A, Shin E, Bauser S, Chen C, Lee D, Shen Y, He Y, Huang MQ. Enhancing magnetic properties of bulk anisotropic Nd–Fe–B/alpha-Fe composite magnets by applying powder coating technologies. IEEE Trans Magn. 2006;42(10):2912.
[39] Choi Y, Jiang JS, Pearson JE, Bader SD, Kavich JJ, Freeland JW, Liu JP. Controlled interface profile in Sm–Co/Fe exchange-spring magnets. Appl Phys Lett. 2007;91(7):072509.
[40] Choi Y, Jiang JS, Pearson JE, Bader SD, Liu JP. Origin of recoil hysteresis loops in Sm–Co/Fe exchange-spring magnets. Appl Phys Lett. 2007;91(2):022502.
[41] Hou Y, Sun S, Rong C, Liu JP. $SmCo_5$/Fe nanocomposites synthesized from reductive annealing of oxide nanoparticles. Appl Phys Lett. 2007;91(15):153117.
[42] Rong CB, Liu JP. Effect of thermal fluctuations on the recoil loops of $SmCo_5$/Fe nanocomposite system. J Appl Phys. 2009; 105(7):07A714.
[43] Rong CB, Zhang Y, Poudyal N, Xiong XY, Kramer MJ, Liu JP. Fabrication of bulk nanocomposite magnets via severe plastic deformation and warm compaction. Appl Phys Lett. 2010; 96(10):102513.
[44] Zhang Y, Kramer MJ, Rong CB, Liu JP. Microstructure and intergranular diffusion in exchange-coupled Sm–Co/Fe nanocomposites. Appl Phys Lett. 2010;97(3):032506.
[45] Chaubey GS, Poudyal N, Liu YZ, Rong CB, Liu JP. Synthesis of Sm–Co and Sm–Co/Fe nanocrystals by reductive annealing of nanoparticles. J Alloys Compd. 2011;509(5):2132.
[46] Liu WQ, Zuo JH, Yue M, Cui ZZ, Zhang DT, Zhang JX, Zhang PY, Ge HL, Guo ZH, Li W. Structure and magnetic properties of bulk anisotropic $SmCo_5$/alpha-Fe nanocomposite permanent magnets with different alpha-Fe content. J Appl Phys. 2011;109(7):07A741.
[47] Rong CB, Zhang Y, Kramer MJ, Liu JP. Correlation between microstructure and first-order magnetization reversal in the $SmCo_5$/alpha-Fe nanocomposite magnets. Phys Lett A. 2011;375(10): 1329.
[48] Rong CB, Zhang Y, Poudyal N, Szlufarska I, Hebert RJ, Kramer MJ, Liu JP. Self-nanoscaling of the soft magnetic phase in bulk SmCo/Fe nanocomposite magnets. J Mater Sci. 2011;46(18): 6065.
[49] Rong CB, Zhang Y, Poudyal N, Wang DP, Kramer MJ, Liu JP. Bulk $SmCo_5$/alpha-Fe nanocomposite permanent magnets fabricated by mould-free Joule-heating compaction. J Appl Phys. 2011;109(7):07A735.
[50] Xiong XY, Rong CB, Rubanov S, Zhang Y, Liu JP. Atom probe study on the bulk nanocomposite SmCo/Fe permanent magnet produced by ball-milling and warm compaction. J Magn Magn Mater. 2011;323(22):2855.
[51] Hu DW, Yue M, Zuo JH, Pan R, Zhang DT, Liu WQ, Zhang JX, Guo ZH, Li W. Structure and magnetic properties of bulk anisotropic $SmCo_5$/alpha-Fe nanocomposite permanent magnets prepared via a bottom up approach. J Alloys Compd. 2012;538:173.
[52] Rong CB, Poudyal N, Liu XB, Zhang Y, Kramer MJ, Liu JP. High temperature magnetic properties of $SmCo_5$/alpha-Fe(Co) bulk nanocomposite magnets. Appl Phys Lett. 2012;101(15): 152401.
[53] Wang DP, Poudyal N, Rong CB, Zhang Y, Kramer MJ, Liu JP. Exchange-coupled nanoscale SmCo/NdFeB hybrid magnets. J Magn Magn Mater. 2012;324(18):2836.
[54] Liu WQ, Zuo JH, Yue M, Lv WC, Zhang DT, Zhang JX. Preparation and magnetic properties of bulk nanostructured $PrCo_5$ permanent magnets with strong magnetic anisotropy. J Appl Phys. 2011;109(7):07A731.
[55] Coey JMD. Hard magnetic materials: a perspective. IEEE Trans Magn. 2011;47(12):4671.
[56] Zhang JJ, Gao HM, Yan Y, Bai X, Su F, Wang WQ, Du XB. Morphology and magnetic properties of $CeCo_5$ submicron flakes prepared by surfactant-assisted high-energy ball milling. J Magn Magn Mater. 2012;324(20):3272.
[57] Li Z, Ding H, Zhang J, Wang HB, Wang H. Effects of annealing temperature and time on microstructure and magnetic properties of Pr–Co thin films. Rare Met. 2012;31(2):121.
[58] Tang CY, Xiao ZY, Luo F, Wang J, Ma CY, Zhang W. Structural characteristics and magnetic properties of bulk nanocrystalline $Fe_{84}Zr_2Nb_4B_{10}$ alloy prepared by mechanical alloying and spark plasma sintering consolidation. Rare Met. 2012;31(3):255.
[59] Liu JJ, Wang R, Yin HY, Liu XC, Si PZ, Du J. Structure and magnetostriction of $Tb_{0.4}Nd_{0.6}(Fe_{0.8}Co_{0.2})_{1.90}$ alloy prepared by solid-state synthesis. Rare Met. 2012;31(6):547.